PHYSICAL REVIEW C VOLUME 52, NUMBER 4 OCTOBER 1995

Neutrino magnetic moment effects in neutrino nucleus reactions

S. K. Singh* and M. Sajjad Athar
Department of Physics, Aligarh Muslim University, Aligarh-202002, India
(Received 7 September 1994)

Some low energy neutrino nucleus reactions induced by neutrinos (antineutrinos) having a magnetic moment of the order of $10^{-9}-10^{-10}$ Bohr magneton are studied. It is found that in the case of ^{4}He, ^{12}C, and ^{16}O, the detection of very low energy scalar and isoscalar elastic and inelastic reactions induced by the isoscalar vector currents can provide a better limit on the neutrino magnetic moment.

PACS number(s): 25.30.Pt, 13.15.+g

I. INTRODUCTION

The neutrino is generally believed to be a massless neutral particle. However, recently the existence of nonzero mass and magnetic moment for the neutrino has been discussed in connection with the solar neutrino problem. Neutrinos with a magnetic moment may interact with the solar magnetic field while passing through the sun and flip their spin, giving rise to wrong helicity, almost sterile neutrinos, thus reducing the solar neutrino flux observed in terrestrial detectors. This requires the neutrinos to have a magnetic moment of the order of $10^{-10}\mu_B$ [1]. This hypothesis also helps to explain the anticorrelation of solar neutrino flux with sun spot cycles [2] and biannual variation of the solar neutrino flux reported in the literature [1]. The nonvanishing value of the magnetic moment for neutrino has many consequences for various processes used in calculating the nucleosynthesis and stellar energy loss mechanisms in astrophysics and cosmology. The upper limits for the neutrino magnetic moment deduced from analyzing these processes are summarized in Table I [3–6].

There have been many attempts to obtain experimental limits on the magnetic moment of neutrinos (antineutrinos) of all species by performing neutrino (antineutrino) electron scattering at various accelerators and reactors. A summary of the existing experimental results is shown in Table I [6–8].

This paper attempts to explore the possibility of finding useful limits, if any, on the neutrino magnetic moment from an analysis of neutrino-nucleus reactions. The first attempt in this direction was made by Reines *et al.* [9] when they observed neutral current reactions on deuterium [10]. Recently, with the observation of neutral current reactions with ν_e and ν_μ beams in ^{12}C, investigation of the possibility of neutrino magnetic moment effects in these reactions was undertaken [11]. It turns out that these reactions in deuterium and ^{12}C [10,11], which are mainly induced by the axial vector currents, do not get any appreciable contribution from the neutrino magnetic moment. We have in this paper looked into the possibility of observing these effects in neutrino nucleus reactions induced by isoscalar vector currents which are suppressed in the standard model. For this purpose, we have considered the elastic and inelastic ($J^P=0^+$, $T=0$) transitions in some nuclei like $^4_2$He, $^{12}_6$C, $^{16}_8$O, $^{40}_{18}$Ar, and $^{98}_{42}$Mo which have been recently proposed in connection with solar neutrino or dark matter detection experiments [6]. Theoretically, elastic reactions are favored as they provide larger cross sections compared to inelastic reactions, but the detection of these reactions, experimentally, is very difficult because of the small recoil of the target nucleus, the only observable in elastic scattering. On the other hand, inelastic reactions are more amenable to experimental detection through the observation of excited state decay products, but are hampered by very small cross sections.

In Sec. II we discuss some general features of weak and electromagnetic scattering of neutrinos with nuclei and derive the various formulas for the differential cross sections and total cross sections corresponding to the elastic and inelastic scattering of neutrinos with a magnetic moment μ and compare with the standard model results. In Sec. III we have numerically evaluated and plotted these cross sections as a function of incident neutrino energy. Here we also present total cross section results for these nuclei after folding with some standard neutrino (antineutrino) spectra from reactors and accelerators and discuss these results. In Sec. IV we conclude our findings.

II. WEAK AND ELECTROMAGNETIC SCATTERING OF NEUTRINOS

The standard model of electroweak interaction describes neutrino scattering with leptons and hadrons through W and

TABLE I. Present upper limits on neutrino magnetic moments.

Constraints	Limits on μ (in μ_B)
Cosmological arguments	
(1) Nuclear synthesis in the big bang [3]	$\mu_{\nu_e}<10^{-11}$
Astrophysical constraints	
(1) Energy loss in He stars [4]	$\mu_{\nu_e}<0.8\times10^{-11}$
(2) Supernova 1987A [5]	$<5\times10^{-10}$
(3) Plasmons in steller plasma [6]	$<(0.1-1)\times10^{-10}$
(4) Stellar cooling [6]	$<10^{-11}$
Laboratory experiments	
(1) $\bar{\nu}_e e$ scattering [7]	$\mu_{\bar{\nu}_e}<4\times10^{-10}$
(2) $\nu_\mu e,\bar{\nu}_\mu e$ scattering [6]	$\mu_{\nu_\mu},\mu_{\bar{\nu}_\mu}<8.5\times10^{-10}$
(3) $\nu_\mu e,\bar{\nu}_\mu e,\nu_e e$ scattering [8]	$\mu_{\nu_e}<10.8\times10^{-10}$
	$\mu_{\nu_\mu}<7.4\times10^{-10}$
(4) ν_τ [7]	$\mu_{\nu_\tau}<4\times10^{-6}$

*Electronic address: Sksphfs@amu.ernet.in

Z exchanges, which are helicity-conserving processes in the case of massless neutrinos. In the presence of nonzero mass of the neutrino, the helicity flipping reactions are also possible whose cross sections are small, being proportional to m_ν^2, where m_ν is the neutrino mass, and are generally quite small. There are no terms linear in m_ν as a result of the absence of interference terms. When the possibility of electromagnetic interactions of neutrinos is considered through the presence of a magnetic moment μ, the scattering processes are helicity flipping. The total electroweak scattering cross sections of the massless neutrino are then the incoherent sum of weak scattering through W,Z exchanges and the electromagnetic scattering through one-photon exchange. In the case of nonzero mass of the neutrino, there is an interference term between the weak and electromagnetic contributions which is linear in mass and magnetic moment of the neutrino. This interference term has been studied and can be shown to be smaller than the other contributions for m_ν about a few keV and $\mu \sim 10^{-10}\mu_B$ [1]. We also find similar results for the elastic and inelastic neutrino nucleus scattering which has been discussed below in Secs. II A and II B.

In addition to the magnetic moment μ discussed above, neutrinos can also have a transition magnetic moment. The electromagnetic neutrino scattering taking place as a result of the transition magnetic moment flips the flavor in addition to flipping the helicity; therefore, it does not interfere with any terms discussed above and the cross section due to this magnetic moment adds incoherently to the above cross sections. The various upper limits quoted for the magnetic moment and reproduced in Table I do not distinguish between these two types of magnetic moments because the experimental neutrino processes do not observe any flavor of the neutrinos in the final state. The quoted upper limits, therefore, apply to both types of magnetic moments. In the following we present the implications of the presence of a nonzero transition magnetic moment of the neutrinos in some neutrino nucleus elastic and inelastic scattering. The results also apply to the case of a normal magnetic moment where the presence of additional interference terms does not affect our results as its contribution is small for the values of nonzero neutrino masses of ν_e and ν_μ, which are consistent with currently available experimental limits [12].

A. Elastic scattering

The form of the matrix element for the neutrino nucleus reaction (with the neutrino magnetic moment μ)

$$\nu(k) + {}^A_Z X(p) \rightarrow \nu(k') + {}^A_Z X(p') \tag{2.1}$$

is written as

$$M_\gamma^T = \mu_T \bar{u}(k')\sigma_{\mu\nu}q^\nu u(k)\frac{ie}{q^2}\langle p'|J_{\rm em}^\mu|p\rangle \ , \tag{2.2}$$

where k and k' are the four-momenta of the incoming and outgoing neutrinos which are of different flavor, p (p') are the incoming (outgoing) four-momenta of the nucleus, q^ν $(=k^\nu - k'^\nu)$ is the four-momentum transfer, μ_T $(=e\mu_\nu/2m_e)$ is the transition magnetic moment of the neutrino, and

$$\langle p'|J_\mu^{\rm em}|p\rangle = (p+p')_\mu F_{\rm el}^{\rm em}(q^2) \ , \tag{2.3}$$

where $F_{\rm el}^{\rm em}(q^2)$ is the nuclear elastic form factor.

From this the following expression for the differential scattering cross section is derived:

$$\frac{d\sigma_{\rm el}^{\rm MM}}{dQ^2} = \frac{\pi\alpha^2 Z^2\mu_\nu^2}{m_e^2 Q^2}\left(1-\frac{p\cdot q}{2ME}\right)^2 F_{\rm el}^{\rm em^2}(Q^2) \ , \tag{2.4}$$

where Z is the atomic number, α is the fine structure constant, E is the incident neutrino energy, M is the mass of the nucleus, and

$$p\cdot q = \frac{Q^2}{2} \ , \tag{2.5}$$

where $Q^2 = -q^2$. The form of the elastic form factor $F_{\rm el}^{\rm em}(Q^2)$ is taken to be $\exp(-aQ^2)$ [13], where a is determined from elastic electron scattering data on various nuclei.

The total cross section as a function of energy is derived to be

$$\sigma_{\rm el}^{\rm MM}(E) = \frac{\pi\alpha^2 Z^2\mu^2}{m_e^2}\left\{\ln\left(\frac{2E^2}{MT_{\rm min}}\right) - 8aE^2 + 16a^2E^4 + \frac{1}{4aME}[\exp(-8aE^2)-1] - \frac{1}{32M^2E^2a}\left[4E^2\exp(-8aE^2) + \frac{1}{2a}[\exp(-8aE^2)-1]\right]\right\} \ , \tag{2.6}$$

where $T_{\rm min}$ is the minimum recoil of the nucleus taken to be zero in all other terms except the logarithmic term. This process takes place in the standard theory of electroweak interactions through the Hamiltonian [14]

$$H = \frac{G_F}{\sqrt{2}}\bar{u}(k')\gamma^\mu(1+\gamma_5)u(k)J_\mu^z \ , \tag{2.7}$$

with the neutral current J_μ^z given by $J_\mu^z = -2\sin^2\theta_W J_\mu^{\rm em}$, where $J_\mu^{\rm em}$ is the electromagnetic current, θ_W is the weak mixing $(\sin^2\theta_W = 0.233)$, and G_F is the Fermi coupling constant. The matrix element, therefore, is written as

$$M_z = \frac{G_F}{\sqrt{2}}\bar{u}(k')\gamma_\mu(1+\gamma_5)u(k)(-2\sin^2\theta_W)(p+p')^\mu F_{\rm el}(Q^2) \ , \tag{2.8}$$

where k and k' now correspond to the four-momenta of initial and final neutrinos of the same flavor.

From this the following expression for the differential scattering cross section is obtained:

$$\frac{d\sigma_{\rm el}^{\rm SM}}{dQ^2}=\frac{2F_{\rm el}^2(Q^2)G_F^2(\sin^2\theta_W)^2Z^2}{\pi}\left(1-\frac{Q^2}{4E^2}-\frac{p\cdot q}{ME}\right) \ . \tag{2.9}$$

The total cross section $\sigma^{\rm SM}(E)$ is then obtained by integrating over Q^2 and is found to be

$$\sigma_{\rm el}^{\rm SM}(E)=\frac{[Z(1-4\sin^2\theta_W)-N]^2G_F^2}{16\pi a}\left[[1-\exp(-8aE^2)]+\left(\frac{1}{2ME}+\frac{1}{4E^2}\right)\left(4E^2\exp(-8aE^2)+\frac{1}{2a}[\exp(-8aE^2)-1]\right)\right] \ . \tag{2.10}$$

The total cross section will be the sum of cross sections given in Eqs. (2.6) and (2.10) as they correspond to final neutrinos of different flavors. However, if the neutrino has a normal magnetic moment μ, then the final neutrino will have the same flavor as the neutrino in Eq. (2.8), for which the matrix element is

$$M_\gamma^N=\mu\bar{u}(k')\sigma_{\mu\nu}q^\nu u(k)\frac{ie}{q^2}\langle p'|J_{\rm em}^\mu|p\rangle \ . \tag{2.11}$$

The differential and total cross sections in this case will be given by Eqs. (2.4) and (2.6) with μ_T replaced by μ and an additional term coming from the interference of M_γ^N and M_z, which is proportional to m_ν and is given by the expressions

$$\frac{d\sigma_{\rm el}^{\rm int}}{dQ^2}=-\frac{m_\nu\alpha G_F\mu_\nu Z^2F_{\rm el}^2(Q^2)\sin^2\theta_W}{\sqrt{2}m_eE^2}\left[1+\frac{p\cdot q}{2M^2}\right] \ , \tag{2.12}$$

$$\sigma_{\rm el}^{\rm int}(E)=-\frac{m_\nu\alpha G_F\mu_\nu Z^2\sin^2\theta_\omega}{2\sqrt{2}m_eE^2a}\left[[1-\exp(-8aE^2)]-\frac{1}{4M^2}\left(4E^2\exp(-8aE^2)+\frac{1}{2a}[-1+\exp(-8aE^2)]\right)\right] \ . \tag{2.13}$$

For a neutrino mass of a few keV and $\mu\sim10^{-13}\mu_B$, $\sigma_{\rm el}^{\rm int}(E)$ becomes comparable to $\sigma_{\rm el}^{\rm MM}(E)$ for $E_\nu\sim10-20$ MeV. For $\mu\sim10^{-10}\mu_B$ used in our present calculations, $\sigma_{\rm el}^{\rm int}(E)$ is quite small in comparison to $\sigma_{\rm el}^{\rm MM}(E)$ and is, therefore, neglected in the subsequent discussions.

B. Inelastic scattering

The form of the matrix element for the neutrino nucleus reaction (with a neutrino magnetic moment μ)

$$\nu(k)+{}_Z^AX(p)\rightarrow\nu(k')+{}_Z^AX^*(p') \ ,$$

where X^* corresponds to the isoscalar-scalar ($J^\pi=0^+$, $T=0$) excited state of the nucleus, is given by (2.2), where the general form of the matrix element $\langle p'|J_\mu^{\rm em}|p\rangle$ is now given by

$$\langle p'|J_\mu^{\rm em}|p\rangle=[F_1(q^2)q_\mu+F_2(q^2)P_\mu] \ , \tag{2.14}$$

where $q_\mu=(p'-p)_\mu$ and $P_\mu=(p'+p)_\mu$. Conservation of electromagnetic current implies that

$$F_2(Q^2)=-\frac{q^2}{q\cdot P}F_1(Q^2) \ . \tag{2.15}$$

Using this value for the matrix element $\langle p'|J_\mu^{\rm em}|p\rangle$ in μ, we get

$$M=\mu\bar{u}(k')\sigma_{\mu\nu}q^\nu u(k)\left(-\frac{ie}{q^2}\right)(p+p')^\mu F_{\rm inel}(Q^2) \ , \tag{2.16}$$

where

$$F_{\rm inel}(Q^2)=\frac{Q^2}{q\cdot P}F_1(Q^2) \ . \tag{2.17}$$

Since $F_{\rm inel}(Q^2)$ vanishes as Q^2 goes to zero [i.e., Eq. (2.4)], experimentally it is parametrized as

$$F_{\rm inel}(Q^2)=Q^2(A+BQ^2)F_{\rm el}(Q^2) \tag{2.18}$$

and the constants A and B are determined from inelastic electron scattering data on various nuclei [15,16].

In the standard model, the matrix element for inelastic neutrino scattering is given by (2.8) except that $F_{\rm el}(Q^2)$ is replaced by $F_{\rm inel}(Q^2)$ as given in (2.18).

From these matrix elements, the following expression for the differential cross section $d\sigma/dQ^2$ and the total cross section σ are obtained for the various cases discussed in Sec. II A:

$$\frac{d\sigma_{\rm inel}^{\rm MM}}{dQ^2}=\frac{\pi\alpha^2\mu^2F_{\rm inel}^2(Q^2)}{m_e^2Q^2}\left[1-\frac{p\cdot q}{2ME}\right]^2 \ , \tag{2.19}$$

$$\frac{d\sigma_{\rm inel}^{\rm SM}}{dQ^2}=\frac{2G_F^2(\sin^2\theta_W)^2F_{\rm inel}^2(Q^2)}{\pi}\left[1-\frac{Q^2}{2E^2}-\frac{p\cdot q}{ME}\right], \tag{2.20}$$

where

$$p\cdot q=\frac{Q^2}{2}+\frac{(M^{*2}-M^2)}{2}, \tag{2.21}$$

and M^* is the mass of the excited nucleus,

$$\sigma_{\rm inel}^{\rm MM}(E)=\left(\frac{2\sqrt{2\pi}\alpha\mu_\nu A}{m_e}\right)^2\sum_{n=0}^{4}\left[a_n+\frac{b_n}{E}+\frac{c_n}{E^2}\right]\times(E-\Delta M)^{n+2}E^{n+2},$$

where

$$a_0=\left(1-\frac{b}{2}-\frac{b^2}{16}\right),\quad b_0=0,\quad c_0=0,$$

$$a_1=\frac{16B}{3A}\left(1-\frac{b}{2}-\frac{b^2}{16}\right),\quad b_1=-\frac{(b+4)}{6M},\quad c_1=0,$$

$$a_2=\frac{8B^2}{A^2}\left(1-\frac{b}{2}-\frac{b^2}{16}\right),\quad b_2=-\frac{(b+4)B}{MA},$$

$$c_2=-\frac{1}{8M^2},$$

$$a_3=0,\quad b_3=-\frac{8(b+4)B^2}{5MA^2},\quad c_3=-\frac{4B}{5M^2A},$$

$$a_4=0,\quad b_4=0,\quad c_4=-\frac{4B^2}{3M^2A^2},$$

$$b=\frac{\Delta M^2}{2EM},\quad \Delta M=M^*-M, \tag{2.22}$$

$$\sigma_{\rm inel}^{\rm SM}(E)=\frac{2(8G_F\sin^2\theta_W A)^2}{3\pi}\sum_{n=0}^{3}\left[a'_n+\frac{b'_n}{E}\right]\times(E-\Delta M)^{n+3}E^{n+3},$$

where

$$a'_0=(1-b),\quad b'_0=0,\quad a'_1=\frac{6B}{A}(1-b),\quad b'_1=-\frac{3a}{2M},$$

$$a'_2=\frac{48B(1-b)}{5A^2},\quad b'_2=-\frac{48aB}{5MA},\quad a'_3=0,$$

$$b'_3=-\frac{16aB^2}{MA^2},\quad a=1+\frac{M}{2E}. \tag{2.23}$$

Other symbols have the same meaning as in Eq. (2.22).

In the case of inelastic scattering, $d\sigma_{\rm inel}^{\rm int}/dQ^2$ is calculated to be similar to Eq. (2.12) with $F_{\rm el}(Q^2)$ replaced by $F_{\rm inel}(Q^2)$ and $p\cdot q$ given by Eq. (2.21). The numerical contribution of $\sigma_{\rm inel}^{\rm int}(E)$, calculated by integrating $d\sigma_{\rm inel}^{\rm int}/dQ^2$, is

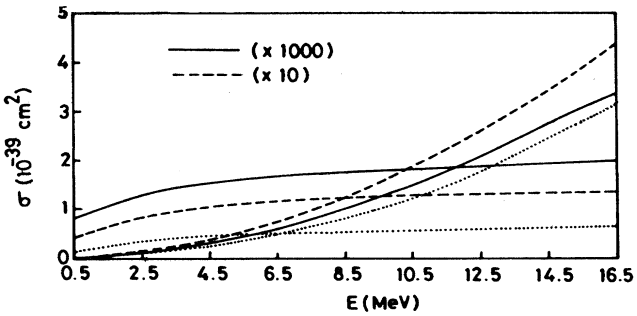

FIG. 1. $\sigma_{\rm el}(E)$ vs E for ^{4}He (solid line), ^{40}Ar (dashed line), and ^{98}Mo (dotted line) targets. The upper curves (a) are for the standard model, while the lower curves (b) are for the case of the magnetic moment with $\mu_{\nu_e}=4\times10^{-10}\mu_B$. Note that different scales have been used for ^{4}He and ^{40}Ar. In the case of ^{12}C and ^{16}O, the nature of the curves is similar to ^{4}He, but an order of magnitude larger.

small in comparison to $\sigma_{\rm inel}^{\rm MM}(E)$ and $\sigma_{\rm inel}^{\rm SM}(E)$ in this case as well and is, therefore, neglected.

III. RESULTS AND DISCUSSION

We have numerically evaluated the total cross sections $\sigma_{\rm el}^{\rm MM}(E)$, $\sigma_{\rm inel}^{\rm MM}(E)$, $\sigma_{\rm el}^{\rm SM}(E)$, and $\sigma_{\rm inel}^{\rm SM}(E)$ using the various formulas given in Sec. II for some nuclei like ^{4}He, ^{12}C, ^{16}O, ^{40}Ar, and ^{98}Mo. These nuclei have been either proposed or are presently being used in various experiments on solar neutrino and astrophysical neutrinos [17]. The proposed bolometric detectors filled with He or LVD detectors filled with ^{12}C or water-based large detectors will be observing many neutrino interactions in the near future [18]. The results from the ambitious ICARUS [19] project using ^{40}Ar and efforts to observe neutrino reactions with ^{98}Mo will also be available sometime in the near future. The energy dependence of the cross section $\sigma(E)$ for neutrino reactions in these nuclei with or without magnetic moments will be useful in analyzing these experiments. In the following we discuss the cases of elastic and inelastic reactions separately.

A. Elastic scattering

The elastic scattering cross sections $\sigma_{\rm el}^{\rm MM}(E)$ and $\sigma_{\rm el}^{\rm SM}(E)$ are evaluated using Eqs. (2.6) and (2.10). In order to calculate these cross sections, we have used the elastic form factors for ^{4}He, ^{12}C, and ^{16}O from the data on elastic scattering and have taken experimental results from [14,16,17].

For ^{40}Ar and ^{98}Mo we have used the charge radii of these nuclei to determine the form factors as defined in (2.3) through the relation $\langle R^2\rangle=-6dF(Q^2)/dQ^2|_{Q^2=0}$. The experimental form of $F(Q^2)=\exp(-aQ^2)$ used for ^{40}Ar and ^{98}Mo should be adequate at very small values of the entire range of Q^2 relevant to energies up to 50 MeV used in our present calculations. In the case of the numerical evaluation of $\sigma^{\rm MM}(E)$, some care has to be taken because of the occurrence of a logarithmic term in Eq. (2.6). Even though the theoretical value of $T_{\rm min}$ is zero, we have substituted $T_{\rm min}=1$ eV to perform the numerical calculations. The values of $\sigma^{\rm MM}(E)$ and $\sigma^{\rm SM}(E)$ calculated in this way are plotted as a function of E and shown in Fig. 1. The numerical

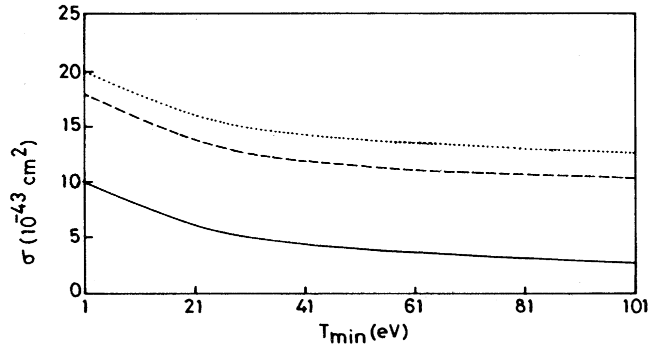

FIG. 2. $\sigma_{el}(E)$ vs T_{min} for ^{4}He at different values of E: $E=1.0$ MeV (solid line), 10.0 MeV (dashed line), and 20.0 MeV (dotted line). In the case of ^{40}Ar, the nature of the curve is similar to ^{4}He, but larger by two orders of magnitude.

values of the cross sections are presented for $\mu=4\times10^{-10}\mu_B$ [7]. We see that at lower energies $\sigma^{MM}(E)$ is larger than $\sigma^{SM}(E)$, but as the neutrino energy E increases, $\sigma^{SM}(E)$ becomes larger than $\sigma^{MM}(E)$. This happens at $E=12$ MeV for ^{4}He, which gradually decreases as we go toward the heavier nuclei. In order to test the sensitivity of our numerical calculations to the assumed value of T_{min}, we have varied T_{min}. The numerical results are shown in Fig. 2, which shows that $\sigma^{MM}(E)$ can vary by factors of 3 at energies relevant to the reactor antineutrinos, while it can vary by factors of 2 at energies relevant to neutrinos from muon decay as we vary T_{min} from 1 to 100 eV. The major problem in observing elastic neutrino scattering is the lack of observables in the final state. The only observable in the final state is the recoil of the target nucleus which is very small. There is a possibility of observing these reactions with the help of bolometric detectors presently being built for various dark matter detection experiments [18]. This introduces an experimental cutoff on T_{min}. For a kilogram size low temperature detector, a T_{min} of 0.1 keV is the best that can be achieved in the near future [10]. If a T_{min} of 0.1 keV is used, then the results quoted in Fig. 1 for $\sigma^{MM}(E)$ will be reduced by a factor of 2–3 over the energy range considered. On the other hand, if the limits of $(0.85-1.08)\times10^{-9}$ as shown in Table I for μ are taken, the numerical results for $\sigma^{MM}(E)$ will be enhanced by a factor of 4–7. This uncertainty should be kept in mind when comparing the values of $\sigma^{MM}(E)$ and $\sigma^{SM}(E)$. To investigate the question whether a deviation in the neutrino cross section from standard model predictions can put useful limits on the neutrino magnetic moment, we have calculated the integrated antineutrino cross sections for two antineutrino spectra taken from Vogel and Engel [2] and Avignone [20] for the purpose of illustration. The total cross sections of Fig. 1, folded with the antineutrino spectra of Vogel and Engel [2] and Avignone [20], are shown in Table II for both cases of $\sigma^{MM}(E)$ and $\sigma^{SM}(E)$. We have also calculated the folded cross section for neutrino scattering for the neutrinos from stopped muon decay [21] and the results are presented in Table III.

TABLE II. Weighted elastic scattering cross sections (in 10^{-41} cm^2) from reactor antineutrinos for different nuclei. Spectra No. 1 from Ref. [20] and spectra No. 2 from Ref. [21].

	Standard model		Magnetic moment	
Nuclei	Spectra No. 1 $\langle\sigma\rangle$	Spectra No. 2 $\langle\sigma\rangle$	Spectra No. 1 $\langle\sigma\rangle$	Spectra No. 2 $\langle\sigma\rangle$
$^4_2$He	9×10^{-3}	5.9×10^{-2}	8.8×10^{-2}	1.0×10^{-1}
$^{12}_6$C	8.1×10^{-2}	5.3×10^{-2}	6.8×10^{-1}	8.1×10^{-1}
$^{16}_8$O	1.4×10^{-1}	9.5×10^{-1}	1.1	1.3
$^{40}_{18}$Ar	1.1	7.4	5.2	6.2
$^{98}_{42}$Mo	7.3	4.8	$2.3\times10^{+1}$	$2.7\times10^{+1}$

TABLE III. Weighted elastic scattering cross sections (in 10^{-38} cm^2) from neutrinos at the accelerators for different nuclei with $\mu_{\nu_\mu}=4\times10^{-10}\mu_B$.

Nuclei	Standard model $\langle\sigma\rangle$	Magnetic moment $\langle\sigma\rangle$
$^4_2$He	2.0×10^{-3}	1.8×10^{-4}
$^{12}_6$C	1.9×10^{-2}	1.0×10^{-2}
$^{16}_8$O	3.4×10^{-2}	1.8×10^{-2}
$^{40}_{18}$Ar	2.6×10^{-1}	1.3×10^{-1}
$^{98}_{42}$Mo	1.7	6.6

B. Inelastic scattering

Neutrino inelastic reactions are experimentally better suited to study the neutrino properties discussed earlier as the decay products of excited states provide additional observables for detection. For example, the 0^+ excited state of ^{4}He decays primarily to proton plus radioactive tritium, while the 0^+ excited state of ^{12}C decays through α emission and the 0^+ excited state of ^{16}O decays by e^+e^- emission. Similarly the 0^+ excited states of ^{40}Ar and ^{98}Mo decay through γ emission and e^+e^- emission, respectively. The disadvantage of these processes is that the calculated cross sections are found to be too small in some cases and are not expected to be observed in the near future. We have, however, calculated them also to give a complete picture of inelastic reactions.

In order to calculate the inelastic cross sections $\sigma^{MM}_{inel}(E)$ and $\sigma^{SM}_{inel}(E)$, we have used Eqs. (2.22) and (2.23). The inelastic form factors $F_{inel}(Q^2)$ are parametrized as in Eq. (2.18). A and B are determined from inelastic electron scattering data on ^{4}He, ^{12}C, and ^{16}O, which are taken from Refs. [14,16,17]. These values are given in Table IV. Using these values of A and B for $F_{inel}(Q^2)$, the total cross sections $\sigma^{MM}_{inel}(E)$ and $\sigma^{SM}_{inel}(E)$ are calculated and plotted as a function of E in Fig. 3. We see that the cross sections are quite small except for ^{4}He where they are appreciable at higher energies.

TABLE IV. Values of A and B.

Nuclei	A (fm^2)	B (fm^4)
$^4_2$He [13]	0.32	−0.06
$^{12}_8$C [15]	0.69	−0.30
$^{16}_8$O [18]	0.26	−0.12
$^{40}_{18}$Ar	0.50	−0.15
$^{98}_{42}$Mo	0.50	−0.15

IV. CONCLUSIONS

We have in this paper analyzed some nuclear reactions induced by neutrinos (antineutrinos) having a magnetic moment of the order of $10^{-10}\mu_B$, which is required theoretically to explain some astrophysical processes and is consistent with the present experimental limits. Earlier investigations in the case of nuclear transitions induced by the isovector axial vector current show negligible effects of the neutrino magnetic moment. In the present case we have investigated some scalar-isoscalar nuclear transitions induced by isoscalar vector currents for some nuclei like ^{4}He, ^{12}C, ^{16}O, ^{40}Ar, and ^{98}Mo. The investigations have been made for low energy high flux neutrino and antineutrino beams relevant at the nuclear reactors as well as for the intermediate energy medium flux neutrino beams available from the muon decays relevant to Los Alamos and Karmen experiments. We find the following.

(i) In the case of neutrino elastic scattering, the magnetic moment contribution to the total cross section $\sigma(E)$ is comparable to the cross section calculated in the standard model at lower energies. However, as the energy increases, the standard model cross section dominates. This happens at about 12.0 MeV for the case of ^{4}He and at lower energies of 11.0 and 10.0 MeV for ^{12}C and ^{16}O, respectively.

(ii) In the case of inelastic scattering, the results are similar to elastic scattering, but the standard model cross section starts dominating over the neutrino magnetic moment contribution very quickly, i.e., 4.0–5.0 MeV above the threshold for ^{4}He and ^{12}C and about 15.0 MeV above the threshold for the case of ^{40}Ar.

(iii) There is the possibility of studying the antineutrino magnetic moment in antineutrino-nucleus scattering at very low energies especially at the reactors in the case of elastic scattering where the cross sections folded over some typical antineutrino spectra at reactors give cross sections of the order of $10^{-41}-10^{-43}$ cm^2. This, however, requires the development of bolometric detectors to detect the very small recoil of the nucleus.

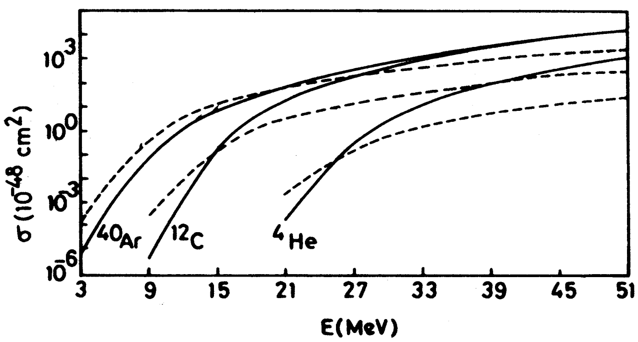

FIG. 3. $\sigma_{\rm inel}(E)$ vs E for inelastic neutrino scattering on ^{4}He, ^{12}C, and ^{40}Ar. The solid lines correspond to the standard model, and dashed curves correspond to the magnetic moment with $\mu_{\nu_e}=4\times10^{-10}\mu_B$ in all cases. In the case of ^{16}O, the energy dependence cross section is similar to ^{12}C, while for ^{98}Mo the cross section is similar to ^{40}Ar.

(iv) At the energies relevant to the Los Alamos and Karmen experiments where ν_μ beams up to 29.8 MeV and ν_e and $\bar{\nu}_\mu$ beams up to 52.8 MeV are available, the neutrino magnetic moment contributions are smaller than the standard model cross section in most cases except for the case of ^{98}Mo.

(v) In the case of inelastic scattering, there is a narrow energy range in which the neutrino magnetic moment contribution is larger than the standard model contribution, but the cross section is too small to be measurable.

We, therefore, conclude that there is the possibility of putting a better limit on the neutrino magnetic moment in neutrino-nucleus reactions provided low energy bolometric detectors are developed to be able to measure the very small recoil energies of nuclei in elastic neutrino-nucleus scattering at low energies.

[1] K. J. F. Gaemers, R. Gandhi, and J. M. Lattimer, Phys. Rev. D **40**, 309 (1989); Chong-Sa Lim and W. J. Marciano, *ibid.* **37**, 1368 (1988); M. B. Voloshin, M. I. Vysotskii, and L. B. Okun, Sov. Phys. JETP **64**, 446 (1986); Sov. J. Nucl. Phys. **44**, 440 (1986); M. Sakuda, Phys. Rev. Lett. **72**, 804 (1994).

[2] P. Vogel and J. Engel, Phys. Rev. D **39**, 3378 (1989); H. Minakata and H. Nunokawa, Phys. Rev. Lett. **63**, 121 (1989).

[3] D. Notzold, Phys. Rev. D **38**, 1658 (1988); J. A. Morgan, Phys. Lett. **102B**, 247 (1981).

[4] D. A. Krakauer *et al.*, Phys. Lett. B **255**, 177 (1990); J. Bernstein, M. Ruderman, and G. Feinberg, Phys. Rev. **132**, 1227 (1963); P. Sutherland *et al.*, Phys. Rev. D **13**, 2700 (1976).

[5] J. M. Lattimer and J. Cooperstein, Phys. Rev. Lett. **61**, 23 (1988).

[6] R. N. Mohapatra and P. B. Pal, *Massive Neutrinos in Physics and Astrophysics* (World Scientific, Singapore, 1989).

[7] D. Fargion *et al.*, Phys. Rev. D **47**, R751 (1993); J. J. Hernandez *et al.*, Phys. Lett. B **239**, 1 (1990).

[8] R. C. Allen *et al.*, Phys. Rev. D **47**, 11 (1993); D. A. Krakauer *et al.*, Phys. Rev. C **45**, 2450 (1992).

[9] F. Reines, H. W. Sobel, and E. Pasireb, Phys. Rev. Lett. **45**, 1307 (1980).

[10] A. C. Dodd, E. Papageorgiu, and S. Ranfone, Phys. Lett. B **266**, 434 (1991).

[11] G. Drexlin *et al.*, Nucl. Instrum. Methods Phys. Res. Sect. A **289**, 490 (1990).

[12] K. Hikasa *et al.*, Phys. Rev. D **45**, 3 (1992).

[13] R. F. Frosch, Nucl. Phys. **A100**, 657 (1968).

[14] J. Bernabeu, S. M. Bilenky, J. Segura, and S. K. Singh, Phys. Lett. B **282**, 177 (1992).

[15] H. Crannel *et al.*, Nucl. Phys. **A90**, 152 (1967).

[16] T. N. Buti *et al.*, Phys. Rev. C **33**, 755 (1986).

[17] J. N. Bahcall, *Neutrino Astrophysics* (Cambridge University Press, Cambridge, England, 1989).

[18] R. E. Lanou *et al.*, Phys. Rev. Lett. **58**, 2498 (1987); J. N. Bahcall, *ibid.* **61**, 2650 (1988); C. Basi *et al.*, Nucl. Instrum.

Methods Phys. Res. Sect. A **264**, 5 (1988); W. C. Haxton, Phys. Rev. D **36**, 2283 (1987); K. Pretzl, N. Schmitz, and L. Stodolsky, *Low Temperature Detectors for Neutrinos and Dark Matter* (Springer-Verlag, Berlin, 1987); A. Drukier and L. Stodolsky, Phys. Rev. D **30**, 2295 (1984).

[19] D. Cline, in *Proceedings of ICNAPP*, Bangalore, 1994, edited by R. Cowsik (World Scientific, Singapore, in press); J. N. Bahcall, M. Baldo-Ceolin, D. B. Cline, and C. Rubbia, Phys. Lett. B **178**, 324 (1986).

[20] H. C. Lee, Nucl. Phys. **A294**, 473 (1978); F. T. Avignone, Phys. Rev. D **2**, 2609 (1970).

[21] M. Pourkaviani and S. L. Mintz, J. Phys. G **16**, 569 (1990); H. Uberall, Nuovo Cimento **23**, 219 (1962).